Soliton self-switching in an asymmetric nonlinear directional coupler

A. K. SARMA
Department of Physics, Indian Institute of Technology Guwahati 781039, India

Soliton switching in an asymmetric nonlinear directional coupler with dissimilar core sizes is studied numerically. A new Schrödinger type coupled nonlinear equations describing the switching dynamics is presented. The relevant coupler parameters are calculated. It is shown that the asymmetric coupler exhibits soliton switching only if the deviation from the symmetry is slight and in the weak coupling regime.

(Received September 10, 2007; accepted October 31, 2007)

Keywords: Soliton, Nonlinear directional coupler, Intermodal dispersion, Nonlinear Schrödinger equation

1. Introduction

Nonlinear directional couplers with cores identical in all respects have been studied extensively in the context of all-optical soliton switching after the pioneering work of Jensen [1], Maier [2] and Trillo, Wabnitz, Wright and Stegeman[3] owing to their use in multitude of fiber-optic devices which require splitting of an optical field into two coherent but physically separated parts [4-13]. Jensen showed that one can switch a continuous signal from one core to the other by varying the input power of the signal. The idea when applied to pulse switching led to pulse distortion and breakup, resulting in inefficient switching. Trillo, Wabnitz, Wright and Stegeman showed that pulse break up could be avoided, if one used soliton pulse as a signal. Recently, nonlinear directional couplers with dissimilar cores have attracted a considerable attention as several new effects can occur in them [14-18]. In this work we are exploring the possibility of soliton switching in an asymmetric NLDC with different core radii. A new pair of coupled nonlinear Schrödinger type equations have been presented and numerically solved to search the possibility of soliton switching.

2. The model

We consider a homogeneous and isotropic nonlinear directional coupler with Kerr nonlinearity, made of two non-identical single-mode fibers with circular cross-sections. Pulse evolution in such a coupler is described by the following set of coupled nonlinear Schrödinger equations (CNLSE), which are derived using the coupled mode theory within the slowly varying envelope approximation [19, 20]:

$$i\left(\frac{\partial A_1}{\partial z}+\frac{1}{v_{g1}}\frac{\partial A_1}{\partial T}+C_{12}^{'}\frac{\partial A_2}{\partial T}\right)+\frac{\beta_{21}}{2}\frac{\partial^2 A_1}{\partial T^2}+C_{12}A_2+\gamma_1|A_1|^2A_1=0 \quad (1)$$

$$i\left(\frac{\partial A_2}{\partial z}+\frac{1}{v_{g2}}\frac{\partial A_2}{\partial T}+C_{21}^{'}\frac{\partial A_1}{\partial T}\right)+\frac{\beta_{22}}{2}\frac{\partial^2 A_2}{\partial T^2}+C_{21}A_1+\gamma_2|A_2|^2A_2=0 \quad (2)$$

Here, A_1 and A_2 are the slowly varying pulse envelopes in large-core (say, core-1) and small-core2 (say, core-2), respectively. $\gamma_i=\frac{n_2\omega_0}{c(A_{eff})_i}; i=1,2$ is the nonlinear parameter, where n_2 is the nonlinear Kerr-co-efficient, c is the speed of light in free space and A_{eff} is known as the effective core area. $\omega_0=\frac{2\pi c}{\lambda}$ is the carrier frequency. The effective core area can be estimated using the formula: $\mathrm{A_{eff}}=\pi r_i^2; i=1, 2$ where r_1 and r_2 are the radii of the 1st and 2nd core respectively. β_{21} and β_{22} are the GVD parameters in the large and the small core respectively, while v_{g1} and v_{g2} are the corresponding group velocities. The coefficients C_{12} and C_{21} are the zeroth-order coupling coefficients between the two cores. They are different because of the difference in the core radii of the coupler. $C_{12}^{'}$ and $C_{21}^{'}$ are the first order coupling coefficient dispersion in core 1 and core-2 respectively, which takes into account the respective intermodal dispersion (IMD) in the two cores.

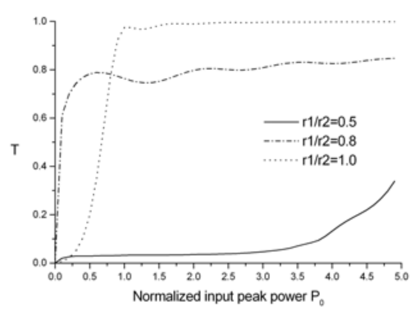

Fig. 1. Plot of the transmission coefficient as a function of the normalized input peak power for soliton of pulse width 30 fs with k_0=0.1 for different radius ratios.

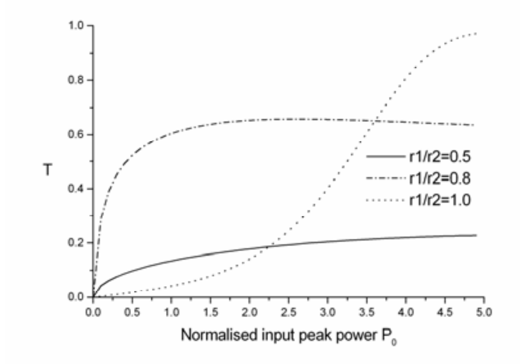

Fig. 2. Plot of the transmission coefficient as a function of the normalized input peak power for soliton of pulse width 30 fs with k_0=0.5 for different radius ratios.

Now, consider a normalized co-ordinate system that moves with the group velocity of the wave at the small-core. Introducing,

$$\xi = \frac{|\beta_{22}|}{T_0^2} z; \tau = \frac{1}{T_0}\left(T - \frac{z}{v_{g2}}\right);$$

$$A_1 = U_1\sqrt{P_0}; A_2 = U_2\sqrt{P_0};$$

$N^2 = \frac{\gamma_2 P_0 T_0^2}{|\beta_{22}|}; u_1 = NU_1$ and $u_2 = NU_2$ Eq.(1) and (2) can be rewritten as

$$i\left[\frac{\partial u_1}{\partial\xi} + \frac{T_0}{\beta_{22}}\left(\frac{1}{v_{g1}} - \frac{1}{v_{g2}}\right)\frac{\partial u_1}{\partial\tau} + \frac{T_0}{\beta_{22}}C_{12}^{'}\frac{\partial u_2}{\partial\tau}\right] + \\ + \frac{1}{2}\frac{\beta_{21}}{\beta_{22}}\frac{\partial^2 u_1}{\partial\tau^2} + \frac{T_0^2}{\beta_{22}}C_{12}u_2 + \frac{\gamma_1}{\gamma_2}|u_1|^2 u_1 = 0 \quad (3)$$

$$i\left[\frac{\partial u_2}{\partial\xi} + \frac{T_0}{\beta_{22}}C_{21}^{'}\frac{\partial u_1}{\partial\tau}\right] + \frac{1}{2}\frac{\partial^2 u_2}{\partial\tau^2} + \frac{T_0^2}{\beta_{22}}C_{21}u_1 + |u_2|^2 u_2 = 0 \quad (4)$$

Again, introducing the normalized parameters in Eq. (3) and (4)

$$\kappa_{01} = C_{12}\frac{T_0^2}{\beta_{21}}; \kappa_{02} = C_{21}\frac{T_0^2}{\beta_{22}}; \kappa_1^{'} = \frac{C_{12}^{'}L_{D1}}{T_0} \text{ and}$$

$$\kappa_2^{'} = \frac{C_{21}^{'}L_{D2}}{T_0} \quad (5)$$

where $L_{D1} = \frac{T_0^2}{\beta_{21}}$ and $L_{D2} = \frac{T_0^2}{\beta_{22}}$ is the dispersion length in the large and small-core respectively, we arrive at the following set of normalized coupled equations:

$$i\left[\frac{\partial u_1}{\partial\xi} + d_{12}\frac{\partial u_1}{\partial\tau} + d_1\frac{\partial u_2}{\partial\tau}\right] + \frac{1}{2}d_{11}\frac{\partial^2 u_1}{\partial\tau^2} + d_{11}\kappa_{01}u_2 + d_n|u_1|^2 u_1 = 0 \quad (6)$$

$$i\left[\frac{\partial u_2}{\partial\xi} + \kappa_2^{'}\frac{\partial u_1}{\partial\tau}\right] + \frac{1}{2}\frac{\partial^2 u_2}{\partial\tau^2} + \kappa_{02}u_1 + |u_2|^2 u_2 = 0 \quad (7)$$

where

$$d_{12} = \frac{T_0}{\beta_{22}}\left(\frac{1}{v_{g1}} - \frac{1}{v_{g2}}\right);$$

$$d_1 = \frac{\beta_{21}}{\beta_{22}}\kappa_1^{'}; d_{11} = \frac{\beta_{21}}{\beta_{22}}; d_n = \frac{\gamma_1}{\gamma_2} \quad (8)$$

3. Coupler parameters

In order to solve Eq. (6) and (7) we need to calculate the values of $v_{g1}, v_{g2}, \beta_{21}, \beta_{22}, C_{12}, C_{21}, C_{12}^{'}$ and $C_{21}^{'}$. $v_{g1}, v_{g2}, \beta_{21}$ and β_{22} can be worked out using the following formulae [21]:

$$\frac{1}{v_{gi}} = \frac{n_2}{c} + \frac{n_1 - n_2}{c}\left[b_i + V_i\frac{db_i}{dV_i}\right] \quad ; i = 1,2 \quad (9)$$

$$\beta_{2i} = \frac{n_1 - n_2}{c}\left[2\frac{V_i}{\omega_0}\frac{db_i}{dV_i} + \frac{V_i^2}{\omega_0}\frac{d^2 b_i}{dV_i^2}\right] \quad ; \quad i = 1,2 \quad (10)$$

where $V_i = \frac{2\pi}{\lambda}n_1 r_i\sqrt{2\Delta}$ is the normalized frequency for the $i-th$ fiber in isolation, r_i is the radius of the $i-th$ core. n_1 is the refractive index of the core, $\Delta \approx \frac{n_1 - n_2}{n_1}$ is the profile height parameter with n_2 as the refractive index of the cladding. b_i is the normalized propagation constant of the $i-th$ fiber which can be estimated from the following empirical formula [21]:

$$b_i = \left(A - \frac{B}{V_i}\right)^2,$$

where

$$A = 1.1428 \text{ and } B = 0.996 \quad (11)$$

It is well known that the coupling co-efficient, apart from the geometry of the waveguides of the coupler, also depends on the core to core separation of the coupler. The zeroth order coupling co-efficient C_{ij} in units of inverse meters is given by [22]

$$C_{ij} = \frac{\sqrt{2\Delta}}{r_i}\frac{U_i^2}{V_i^3}\frac{K_0(\frac{a}{r_i}W_i)}{K_1^2(W_i)}, \quad i,j=1,2; i \neq j \quad (12)$$

where r_i is the core radius and a is the centre to centre separation between the cores of the coupler. K_0 and K_1 are the modified Bessel functions. The core and cladding parameters V, U and W are given by

$V_i = \frac{2\pi}{\lambda} n_1 r_i \sqrt{2\Delta}$, $U_i = \sqrt{1 + 2\ln V_i}$ and $W_i = \sqrt{V_i^2 - U_i^2}$, where n_1 is the refractive index of the core. In order to obtain $C_{ij}^{'}$ we need to calculate $\frac{dC_{ij}}{d\omega}\Big|_{\omega=\omega_0}$. Introducing the auxiliary function

$$G_i = [2 + 2W_i\frac{K_0(W_i)}{K_1(W_i)} - W_i\frac{a}{r_i}\frac{K_1(W_i\frac{a}{r_i})}{K_0(W_i\frac{a}{r_i})}]\times[1+\frac{U_i^2}{W_i^2}\frac{K_0^2(W_i)}{K_1^2(W_i)}] - [1+\frac{2K_0^2(W_i)}{K_1^2(W_i)}] \quad (13)$$

We may write

$$C_{ij}^{'} = \frac{\sqrt{2\Delta}}{\omega_0 r_i}\frac{U_i^2}{V_i^3}\frac{K_0(\frac{a}{r_i}W_i)}{K_1^2(W_i)}G_i. \quad (14)$$

Using Eq. (9)-(14) we can calculate all the required parameters we need to solve Eq. (6) and (7). For our calculations we are using the following typical parameters: $n_1 = 1.45; \Delta = 0.004; \lambda = 1.55\mu m$ and nonlinear refractive index $n_2 = 2.6 \times 10^{-20} m^2/W$.

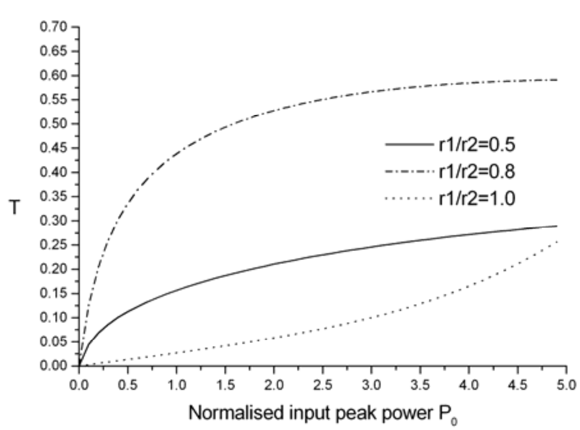

Fig. 3. Plot of the transmission coefficient as a function of the normalized input peak power for soliton of pulse width 30fs withk_0=0.5 for different radius ratios.

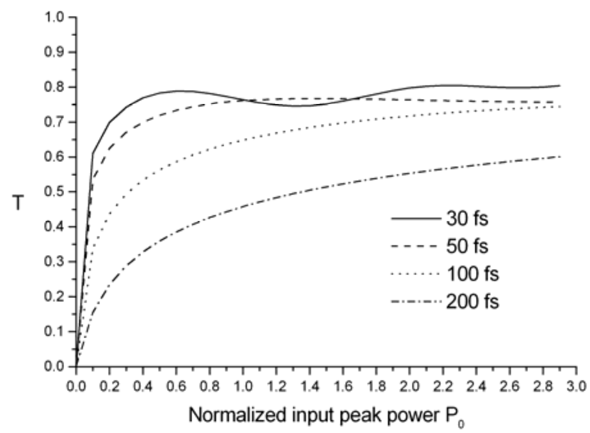

Fig. 4. Plot of the transmission coefficient as a function of the normalized input peak power for different soliton pulse width with k_0=0.1 at r_2=0.8r.

A very important coupler parameter is the so called normalized coupling length ξ_C which is generally defined, in the context of a $\frac{\pi}{2}$ linear coupler, as the length ξ at which the power completely transfers from the input fiber to the other fiber. If we take the large core as our input fiber then from Eq. (6) and (7) it can be shown very easily that

$$\xi_C = \frac{\pi}{2\sqrt{d_{11}\kappa_{01}\kappa_{02}}} = \frac{\pi}{2\kappa_0},$$

where $\kappa_0 = \sqrt{d_{11}\kappa_{01}\kappa_{02}}$ (15)

4. Results and discussion

As the equation (7) with (8) is not analytically solvable, we solve them numerically by the so called split-step Fourier method. The linear dispersive part is solved by the fast Fourier transform method and the nonlinear part is solved by the fourth- order Runge-Kutta method with auto-control of the step size for a given accuracy of the results. For a detailed discussion on the split-step Fourier method the readers are referred to ref.19, chap.2.

We calculate the transmission co-efficient T, representing the fractional output energy in core 1, according to the formula

$$T = \frac{\int_{-\infty}^{\infty}|u_1(\xi,\tau)|^2 d\tau}{\int_{-\infty}^{\infty}\left(|u_1(\xi,\tau)|^2 + |u_2(\xi,\tau)|^2\right)d\tau} \quad (16)$$

In this work we have calculated the transmission coefficient T at end of one coupling length of the coupler as defined in section 3.

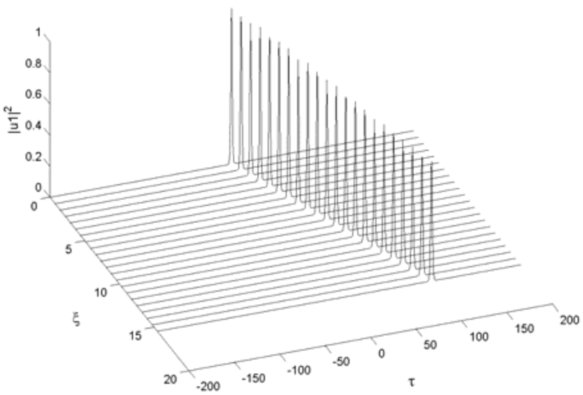

Fig. 5. (a) Spatio-temporal evolution of a 30 fs soliton pulse inside the coupler in core1 with k_0=0.1 and p_0=1.

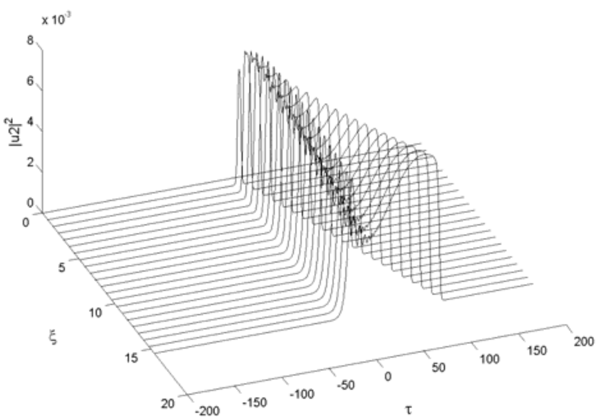

Fig. 5. (b) Spatio-temporal evolution of the small radiation in core2 with k_0=0.1 and p=1.

To analyze the switching process we consider the following initial conditions

$$u_1(0,\tau)=\sqrt{p_0}\,\mathrm{sec}\,h(\sqrt{p_0}\,\tau),\quad u_2(0,\tau)=0, \tag{17}$$

In this work the results are presented for κ_0 equal to 0.1, 0.5 and 1.0. They, in our convention, correspond to weak coupling, moderate coupling and strong coupling, respectively. Fig. 1-3 shows the transmission characteristics of the asymmetric coupler for different radius ratios for κ_0 equal to 0.1, 0.5 and 1.0 respectively. $r_1 = r_2$ corresponds to the case of symmetric coupler. It can be quite clearly observed from the plots that deviation from the symmetry results in the considerable reduction of the critical power of switching, the power at which 50-50 energy sharing takes place between the cores of the coupler. But this deviation in symmetry also results in the reduction of transmittivity. Therefore a trade-off between the critical power and transmitivity is required. We observe that the best bet is offered by $\kappa_0 = 0.1$ at $r_1 = 0.8r_2$. In fact we observe that both the moderate and strong coupling regime do not show switching at all when the geometry of the coupler deviates from the symmetric one. Therefore, now onwards we would study the coupler characteristics for $\kappa_0 = 0.1$ at $r_2 = 0.8r_1$ only. In order to study the effect of the pulse width variation on the transmission of the coupler, in Fig.4 we plot the variation of the transmitivity of the coupler with normalized input peak power for different pulse widths. We observe that with increase in the pulse width the transmitivity decreases and the critical power of switching increases. So it is better to use shorter pulse. Now in order to check the stability and behavior of the soliton pulse inside the coupler, the evolution of the soliton pulse inside core1 is depicted in Fig.5 (a). On the other hand, Fig.5 (b) shows the evolution of a small radiation in core-2 of the couper.It can be seen quite clearly that the solitonic nature of the pulse is completely maintained in core-1 of the coupler. Hence we can conclude that soliton switching can be achieved in the proposed asymmetric coupler with given configuration.

5. Conclusions

We have carried out a detailed numerical study of soliton switching in an asymmetric nonlinear directional coupler with dissimilar cores. A new Schrödinger type coupled nonlinear partial differential equations representing the switching dynamics in the asymmetric coupler is presented. The relevant coupler parameters are calculated to study the new coupled equations numerically. It has been found that the coupler shows switching characteristics only in the weak coupling regime. Moreover, the coupler exhibits soliton switching only if the deviation from the symmetric configuration is very slight. Large deviation from the symmetry forbids soliton switching even in the weak coupling regime.

References

[1] S. M. Jensen, IEEE J. Quantum Electron. QE-**18** , 1580(1982).
[2] A. A. Maier, Kvant. Electron. (Moscow) **9**, 2296(1982)
[3] S. Trillo, S. Wabnitz, E. M. Wright, G. I. Stegeman, Opt. Lett. **13**, 672(1988).
[4] C. Paré, M. Florjańczyk, Phys. Rev. A **41**, 6287(1990).
[5] P. M. Ramos, C. R. Paiva, IEEE J. Quantum Electron, QE-**35**, 983(1999).
[6] Ajit Kumar, Amarendra K. Sarma, Opt. Commun. **234**, 427(2004).

[7] Y. Wang, W. Wang, Journal of Lightwave Technology **24**, 1041(2006).
[8] Y. Fang, J. Zhou, Opti*k*, (in press) (2006).
[9] Ajit Kumar, Amarendra K.Sarma, Japanese Journal of Applied Physics **44**, 8498(2005).
[10] Theo P. Valkering, Joost van Honschoten, Hugo J. W. M. Hoekstra, Opt. Comm. **159**, 215 (1999).
[11] Sotiris Droulias, Manos Manousakis, Kyriakos Hizanidis, Opt. Comm. **240**, 209 (2004).
[12] I. M. Skinner, G. D. Peng, B. A. Malomed and P. L.Chu**.** Opt. Commun.**113**, 493(1995).
[13] B. A.Umarov, F. Kh. Abdullaev, M. K. B. Wahiddin. Opt. Commun. **162**, 340(1999).
[14] P. Shum, M. Liu, IEEE Photonics Technology Letters **14**, 1106 (2002).
[15] B. A. Malomed, Phys.Rev.E 51, R864 (1995).
[16] B. A. Malomed, I. M. Skinner, P. L. Chu, G. D. Peng, Phys. Rev.E **53**, 4084 (1996)
[17] D. J. Kaup,T. I. Lakoba, B. A. Malomed, J. Opt. Soc. Am. B **14**, 1199 (1997).
[18] D. J. Kaup, B. A. Malomed, J. Opt. Soc. Am. B **15**, 2838 (1998).
[19] G. P. Agrawal, Nonlinear Fiber Optics, second ed.(Academic Press, New Work, 2000).
[20] G. P. Agrawal, Application of Nonlinear Fiber Optics, second ed. (Academic Press, New Work, 2000).
[21] A. Ghatak, K. Thyagarajan, Introduction to Fiber Optics (Cambridge University Press, 2002).
[22] A. W. Snyder, J. D. Love, Optical waveguide theory (Chapman and Hall, London, 1983) Chaps. 12-15.

*Corresponding author: aksarma@iitg.ernet.in